Collective microwave scattering diagnostic on the H-1 heliac

W. M. Solomon, M. G. Shats, D. Korneev,[a] and K. Nagasaki[b]
Plasma Research Laboratory, Research School of Physical Sciences and Engineering, Australian National University, Canberra ACT 0200, Australia

(Presented on 19 June 2000)

A multichannel microwave scattering diagnostic has been developed and installed on the H-1 heliac. The purpose of the new diagnostic is to study small-scale plasma fluctuations in H-1, which are believed to be responsible for the loss of particles and energy from the plasma. The diagnostic is a 132 GHz, four-channel superheterodyne system. The transmitter and receiver antennas (consisting of horns and focusing bispherical mirrors) are located inside the vacuum vessel of H-1. A radial resolution of $\Delta r/a \sim 0.2$ is achieved. The scattering volume is positioned in the density gradient region at $r/a \sim 0.6$. At present, the system is aligned to measure fluctuations in the poloidal wave number range from approximately 10 to 25 cm^{-1}. The use of the heterodyne detection system allows the fluctuation propagation direction to be determined. The low frequency bandwidth of the system is 1 MHz. The instrument sensitivity is about $P_s/P_i \sim 10^{-6}$. [DOI: 10.1063/1.1315635]

I. INTRODUCTION

A multichannel microwave scattering diagnostic has been developed and installed on the H-1 heliac.[1] Microwave scattering has been used to study small-scale fluctuations in both tokamaks[2–4] and stellarators.[5] These fluctuations are among candidates for anomalous transport in magnetically confined plasmas.

The diagnostic is a four-channel superheterodyne system, which has a carrier microwave frequency of 131.8 GHz. The transmitter power is 50 mW. It boasts good spatial resolution and wave number selectivity and is sensitive down to −60 dB.

Electromagnetic radiation of wave vector $\boldsymbol{k}_i$ and frequency ω_i is incident on the plasma and is scattered by an electron density fluctuation of wave vector $\boldsymbol{k}$ and frequency ω. The scattered radiation is characterized by a wave vector $\boldsymbol{k}_s$ and frequency ω_s:

$$\boldsymbol{k}_s = \boldsymbol{k}_i \pm \boldsymbol{k}, \quad \omega_s = \omega_i \pm \omega. \tag{1}$$

Provided $\omega \ll \omega_i$ then the wave number of the scattered radiation scattered by an angle θ is given by the Bragg condition

$$k = 2k_i \sin(\theta/2). \tag{2}$$

Equation (2) illustrates that a fixed angle of scattering provides good k selectivity. In Sec. II, the geometry of the system as it is set up in H-1 is described. The hardware associated with the system is detailed in Sec. III and in Sec. IV some noise analysis of the scattering system is presented.

[a]Permanent address: ELVA-1, Millimetre Wave Division, 74 Nevsky Pr., 23N, St. Petersburg.
[b]Permanent address: Institute of Advanced Energy, Kyoto University, Japan.

II. SYSTEM GEOMETRY

The setup of the diagnostic is shown in Fig. 1. The microwave power is launched from the bottom (transmitter) horn and focused into the plasma. The four receivers are aligned so as to detect scattering angles of 20°, 30°, 45°, and 55°. According to Eq. (2), this corresponds to k numbers of approximately 10, 14, 21, and 25 cm^{-1}, respectively. In particular, the alignment is such that the dominant component of k is in the poloidal direction. In the actual geometry on H-1 we measure the k selectivity of each channel to be better than $\Delta k < 0.2\ \text{cm}^{-1}$. The k spectra of the density fluctuations will

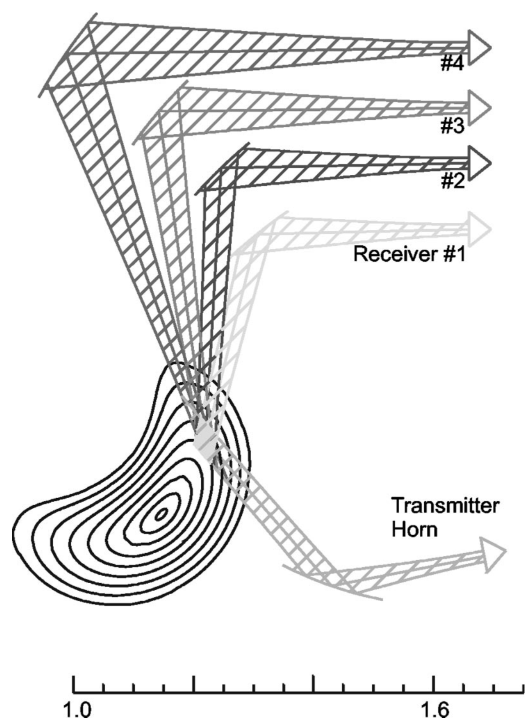

FIG. 1. Schematic of diagnostic setup.

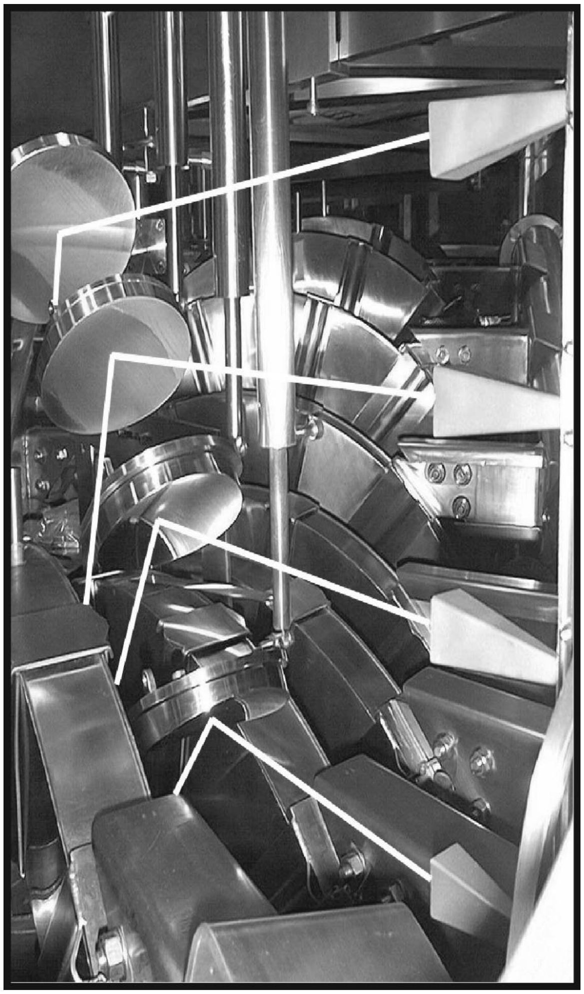

FIG. 2. Photograph showing antenna system as installed inside the vacuum vessel of H-1.

be reconstructed from these four sampled positions in k space. The microwave scattering diagnostic is designed to characterize broadband turbulence. Only in these conditions is it meaningful to try to reconstruct the turbulence k spectrum from the four wave number channels of the diagnostic.

The scattering volume, which is defined as the intersection of radiation patterns of transmitter antenna and receiver antenna, is located at $r/a \sim 0.6$. The radial resolution $\Delta r/a$ for each channel is approximately 0.2. This corresponds to a scattering volume in the plasma no larger than a cube of side 2 cm. The scattering volume is calculated using a Monte Carlo technique using the measured profiles of the transmitter and receiver microwave beams.

The diagnostic will be operated in plasma with a maximum expected density of about $6 \times 10^{18}\,\mathrm{m}^{-3}$. Under these conditions, the transmitter frequency is well above the cutoff frequency. Ray tracing code[6] using realistic density profiles indicates that the refraction effects are negligibly small.

III. HARDWARE

Figure 2 shows the actual setup of the diagnostic. The antenna system is entirely contained in the vacuum tank of H-1. The microwave horns of the four receiving antennas are

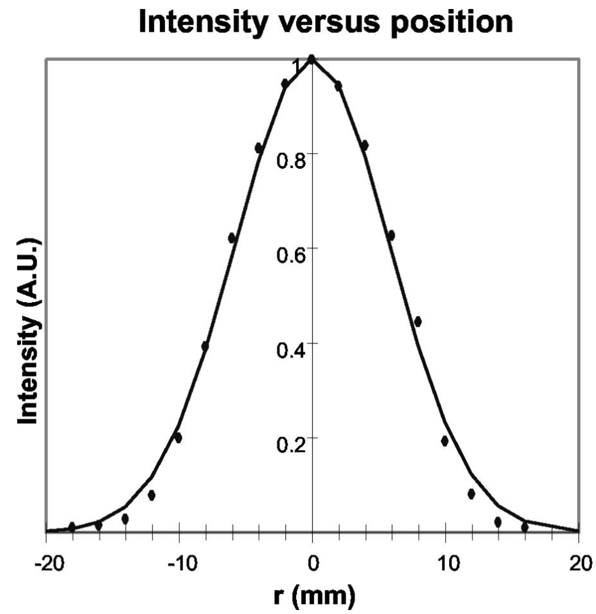

FIG. 3. Measured microwave beam profile (diamonds) and calculated Gaussian (solid) of antenna at the focal position.

located to the right of the figure and the focusing mirrors are towards the left. The diagnostic is aligned in a poloidal plane located between a pair of toroidal field coils.

The antenna system consists of five rectangular horns and five focusing mirrors. The circular mirrors are manufactured from stainless steel and are quasioptical, bispherical mirrors. Apart from their primary purpose of focusing, the mirrors provide a form of spatial filtering of the Gaussian microwave beams.

The mirror–horn combinations produced good Gaussian profiles as shown in Fig. 3. The full width at half maximum (FWHM) of this intensity profile is approximately 14 mm. All mirrors focus the microwaves down to FWHMs of <20 mm. Profiles were measured at various propagation distances, thus providing a measure of beam width as a function of distance. The shaded areas in Fig. 1 are interpolations of the measured beam widths for each antenna.

The detection system uses Impatt semiconductor microwave sources for the transmitter and local oscillators. The schematic in Fig. 4 represents the detection system. The phasing between the transmitter and receivers is centrally managed by a synchronizer unit. The synchronizer uses a

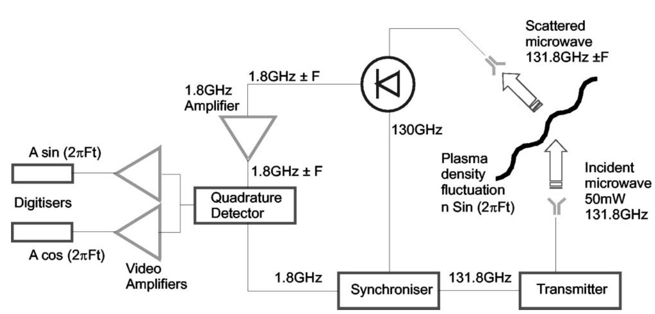

FIG. 4. Schematic of detection process from transmitter, to plasma density fluctuation, to receivers and digitizers.

reference crystal oscillator and a transistor oscillator to produce three signals of frequencies 1.8, 130, and 7.32 GHz.

The 7.32 GHz is sent to the transmitter, where amplification and frequency multiplication produces about 50 mW of microwave power at 131.8 GHz. This wave is launched into the plasma and is scattered by a density fluctuation to one of the receiving channels. The frequency of the scattered wave is Doppler shifted by density fluctuations to $131.8\,\mathrm{GHz}\pm F$. The $\pm F$ results from a fluctuation of frequency F, with the sign indicative of the direction of the propagating fluctuation. The heterodyne detection retains this information on the direction.

The scattered wave is passed to the first mixer in the receiver, where it is mixed with the 130 GHz signal from the synchronizer. The output of the mixer is then $1.8\,\mathrm{GHz}\pm F$. After further amplification, the remaining 1.8 GHz signal from the synchronizer is mixed at the quadrature detector, producing the desired $\pm F$ signal. This is output in terms of its sine and cosine components, namely

$$x=A(t)\cos\phi(t),$$
$$y=A(t)\sin\phi(t), \quad (3)$$

where $A(t)$ represents the amplitude of the fluctuation and $\phi(t)=2\pi F(t)\times t$.

These signals are then sent to the digitizers for processing. The video amplifier bandwidth is 1 kHz–1 MHz.

The signals (3) from the quadrature detector can be combined together into a single complex signal.

$$z=x+jy=A(t)\exp(\phi(t)). \quad (4)$$

Using standard procedures, we can determine the power spectrum of the signal.[7]

$$S_z=S_{xx}+S_{yy}+j(S_{xy}-S_{yx}), \quad (5)$$

where S_{xx} and S_{yy} are the auto power spectra of the two signals *x* and *y*, and S_{xy} and S_{yx} are the cross power spectra.

The effect of using two signals is shown in the $S_{xy}-S_{yx}$ term, which generates an asymmetry in the spectrum around frequency $F=0$. This asymmetry is used to determine the direction of propagation.

IV. NOISE ANALYSIS AND DIAGNOSTIC SENSITIVITY

The stray radiation level is an important factor affecting the diagnostic sensitivity.[8] Stray radiation refers to microwaves that contaminate a scattered signal. It usually occurs as a result of forward (small angle) scattering, followed by multiple reflections from surfaces inside the vacuum chamber. Thus, information about the plasma fluctuations is contained in the stray radiation and is not removed in the heterodyne process. Measuring the stray radiation must be done *in situ* to account for the internal reflections.

Measurements of the stray radiation in H-1 have been made first in the absence of plasma. To increase the measurement sensitivity, the input microwave power was 100% amplitude modulated at 5 kHz.

A large, rotatable planar mirror was placed inside the vacuum tank with its rotation axis at the position of the scattering volume. The throughput power was measured for each channel by directing the microwave radiation with the planar mirror. A diode detector suitable for measuring the full throughput power was used in place of the receivers.

The planar mirror was then removed from the system and the measurements were repeated using the detector with a narrow band (centered around 5 kHz) amplifier of gain 10^4. This measurement provides a realistic estimate for the stray radiation of the system. The stray radiation was below the detectable level of the detector and was inferred to be below -50 dB of the throughput power on all channels. This then represents an upper limit for the stray radiation in the system. When the detector was replaced with the heterodyne receivers, the stray radiation signals are found to be about a factor of ten above the instrument noise.

The frequency content of the stray radiation has been measured during plasma experiments. Comparison with Langmuir probes is possible due to the relatively low electron temperature $\sim$10 eV. The probes are sensitive to wave numbers $k<40\,\mathrm{cm}^{-1}$. In the low confinement mode as described in Ref. 9, the spectrum is found to be dominated by low wave number fluctuations ($k_{\mathrm{pol}}\sim 0.15\,\mathrm{cm}^{-1}$) as measured by probes. The lowest k that we can detect with the microwave scattering diagnostic is 10 cm^{-1}, therefore in this mode of operation, we do not expect to observe direct scattering and signals detected by the diagnostic are a result of stray radiation. Measurements in the low confinement mode provide a means to measure the stray radiation in the plasma experiments. Density fluctuations in the region of the scattering volume are typically around 30%. The level of the stray radiation was found to be about three times lower than the upper limit described above. Using the upper limit of the stray radiation estimate, the system sensitivity to density fluctuations is no worse than $\tilde{n}/\bar{n}<0.3\%$. In the high mode of confinement, the observed fluctuations in the plasma as measured by the probe are reduced by more than an order of magnitude. The same reduction in the fluctuation-produced stray radiation is observed with the microwave scattering system.

ACKNOWLEDGMENT

The authors are grateful to J. Wach for technical support provided during the installation of the microwave scattering diagnostic.

[1] S. M. Hamberger, B. D. Blackwell, L. E. Sharp, and D. B. Shenton, Fusion Technol. **17**, 123 (1990).
[2] E. Mazzucato, Phys. Fluids **21**, 1063 (1978).
[3] D. L. Brower, W. A. Peebles, and N. C. Luhmann, Jr., Rev. Sci. Instrum. **57**, 1977 (1986).
[4] M. Jadoul, G. Waidmann, and P. E. Vandenplas, Plasma Phys. Controlled Fusion **40**, 381 (1998).
[5] M. G. Shats *et al.*, Phys. Plasmas **2**, 398 (1995).
[6] K. Nagasaki, M. G. Shats, H. Smith, and H. Punzmann, J. Phys. Soc. Jpn. (submitted).
[7] O. Asada, A. Inoue, and T. Tsukishima, Rev. Sci. Instrum. **51**, 1308 (1980).
[8] N. Bretz, R. Nazikian, W. Bergin, M. Diesso, J. Felt, and M. McCarthy, Rev. Sci. Instrum. **61**, 3031 (1990).
[9] M. G. Shats, Plasma Phys. Controlled Fusion **41**, 1357 (1999).